PAPER E

New Approach to Improve the Piezoelectric Quality of ZnO Resonator Devices by Chemomechanical Polishing

In: The Nano-Micro Interface: Bringing the Micro and Nano Worlds Together. Edited by H.-J. Fecht and M. Werner. Weinheim: Wiley-VCH. 2004. Pp. 181–193.

WILEY-VCH K+V Fotosatz GmbH
Fecht/Werner Beerfelden
1. UK 22.7.2004
C. Grössl

New Approach to Improve the Piezoelectric Quality of ZnO Resonator Devices by Chemomechanical Polishing

J. Molarius, M. Kulawski, T. Pensala, and M. Ylilammi Q1

1 Introduction

The main application for FBARs is in telecommunications, especially in mobile phones. There is an ever-ongoing development of making smaller and smarter mobile phones than before. One phone should be able to work around the world on different frequencies, which of course increases the number of filters needed in a given phone. The number of RF filters in a mobile phone ranges from three to seven, which results in world market of about 2 billion pieces per year [1]. Because of the big size of the telecommunications market also the research activity around the world on the subject of FBAR has recently been high [1–6]. There are two ways to make phones smaller; shrinking the size of individual devices and increasing integration. FBAR in the current form achieves the first goal by its capability to produce very small, thin, and light filters. Comparison with the current market leaders of surface acoustic wave filters shows that FBAR filters have steeper filter skirts, smaller temperature coefficient of frequency (TCF), smaller chip size and better power handling capability [1, 6]. All these differences are significant, and furthermore the comparison is between mature SAW technology and the first generation of commercial FBAR devices: SMR type (solidly mounted resonator, see below) or bridge type. FBAR also gives good promise for future integration with RF circuits as materials, processing, and thermal budget can easily be designed to be compatible with CMOS processing, for example. The FBAR structure lends itself also to other applications (gas- and pressure-sensors have been suggested). The performance of these sensors using ZnO as piezolayer and SMR type structure with mirrors has been calculated and found to be excellent [7].

There are two basic FBAR structures; namely bridge (also called membrane) resonators or solidly mounted (also called mirror) resonators. The piezoelectric layer is vibrating between two electrodes and in bridge type device the substrate and the resonator are decoupled by an air gap. The air gap, in principle, provides almost ideal isolation, but in practice the lower electrode as well as the supporting structure cause losses. The bridge structure has been utilized to make filters using the resonators in a ladder configuration [5]. Bridges or membranes are

The Nano–Micro Interface: Bringing the Micro and Nano Wolds Together.
Edited by Hans-Jörg Fecht and Matthias Werner

ISBN: 3-527-30978-0

usually made by surface (or bulk) micromachining, which is often considered limiting the yield and productivity. Nevertheless there is a commercial producer for bridge-type FBAR passband filters for frequencies around 2 GHz [6].

Mirrors for isolating the resonator from the substrate was first proposed by Newell [8] in 1965 and then 30 years later developed to modern SMR structure by Lakin [9]. Here the resonator is isolated from the substrate by an acoustical mirror, build from alternating layers of high and low acoustical impedance materials, whose thicknesses are a quarter of the acoustic wavelength at the operation frequency. Depending of the choice of materials typically two to four layer pairs are needed. If molybdenum is used as the high impedance material and SiO_2 as the low impedance material three layer pairs are needed, but substituting Mo with W, two pairs are sufficient for adequate resonator substrate isolation. Mirrors can also be made of completely insulating materials such as AlN and SiO_2, which would give the benefit of easier processing as the mirror would not need any patterning. Metals in the mirror layers need patterning otherwise the parasitic capacitances associated with the conductive metal layers would cause problems in the device operation. Heavy metals have a high acoustic impedance and a high acoustic reflectivity, but a mirror made of AlN/SiO_2 requires four reflective pairs.

For making devices using bulk acoustic waves the quality of the piezolayer is paramountly important. In this chapter we are concentrating on ZnO, but same is true to other piezoelectric materials such as AlN or PZT {$Pb(ZrTi)O_3$}. Zinc oxide is chosen because of its high acoustic coupling coefficient ($k_{mat}=0.282$, $k^2=7.95\%$) [5]. Lead zirconate titanate PZT promises the highest coupling coefficient at 0.28–0.5, after annealing, but very low Q-values (only 18 at 2.3 GHz) [3]. Aluminum nitride AlN on the other hand has a smaller temperature coefficient of
Q2 frequency (TFE) ($\sim$25 ppm) than zinc oxide ($\sim$50 ppm). The smaller TFE of AlN in some FBAR filter applications can nullify the benefit of the higher acoustic coupling coefficient of ZnO. The longitudinal sound velocity in AlN is 10 400 m/s, which is over 60% higher than in ZnO, 6400 m/s. As the thickness of the piezolayer largely determines the frequency of the device, it is advantageous, at low frequencies, to have low sound velocity as the films will be thinner and therefore faster to deposit resulting in increased productivity. At high frequencies, the effective coupling becomes low with a piezomaterial with a low sound velocity because of the small thickness of the layer. This would indicate that ZnO is better at low frequencies and AlN at high frequencies.

The most important parameter determining the quality of piezoelectric layer (AlN or ZnO) is a strong preferred orientation of the film. For FBAR devices operating in the longitudinal wave mode this is (0001). As the crystal is thus growing c-axis perpendicular to the substrate the hexagonal basal plane is interacting with the seed layer. ZnO films can and have been deposited by several different ways, such as CVD (chemical vapor deposition), laser ablation, and PVD methods (physical vapor deposition). In the PVD methods magnetron sputtering, either by rf-sputtering from ZnO-target or by dc or pulsed dc in reactive mode from zinc target in oxygen containing atmosphere, have been extensively used as the temperatures remain low during deposition and there is good compatibility with standard semiconductor device processing. Beside the sputtering parameters themselves, other issues affecting the piezoelectric film quality are the seed layer and the sputtering environment (affecting contamination). If the seed layer is used as the bottom electrode of the device, it has to be highly conducting to keep the electrical losses to a minimum. Therefore it is advantageous to separate these functions to a highly conducting bottom electrode and to a separate seed layer, which can be optimized to promote piezolayer growth and acoustical properties of the FBAR stack. Device quality ZnO can be grown on several metals, at VTT this has been realized on gold and molybdenum [4, 5, 10, 11]. It has been shown that good quality AlN, which has the same wurtzite-type crystal structure as ZnO, can be grown on different seed materials [12]. Löbl [13] and S.-H. Lee [14] for AlN and J. B. Lee [15] for ZnO identified the surface roughness of the seed layer as the decisive factor on piezoelectric film quality; the smoother the seed layer, the better the piezoelectric film quality. The film quality was measured by X-ray rocking curve of ZnO film and the FWHM (full width half maximum) of the (0002) peak was shown to correlate with the effective acoustic coupling coefficient, k_{eff} [3]. K_{eff} on the other hand determines the bandwidth and insertion loss of a filter [16]. Quality factors, Q, are determined at both series and parallel resonance. They are calculated according to the IEEE standard [17]. The reason for the correlation between surface roughness and film quality is quite simple. Since the deposition takes place at low temperature and with low particle energy, adatoms on the surface have low mobility and they do not reach the energetically favored positions for the growth in the preferred orientation. On a smooth substrate the movement of the adatoms is easier and this results in improved piezolayer quality. Control of the surface roughness of a given metal can only be achieved to a certain degree with adjustment of the sputtering parameters, as other film properties, especially stresses in the film, will also be strongly affected. Therefore a better approach is needed.

CMP is usually used to planarize device structures, as seen in the diagram in Fig. 1. The wafer is held on a carrier and pressed with a defined force against a micro-porous polyurethane polishing cloth, which is glued on the rigid polishing

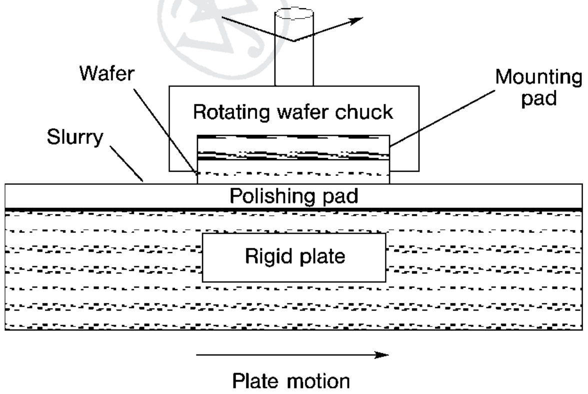

Fig. 1 Diagram of chemomechanical polishing (CMP).

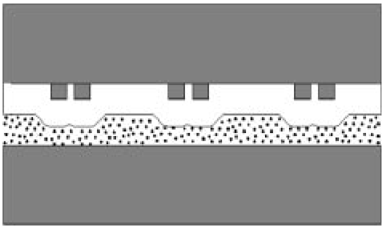

Fig. 2 Principle of CMP removal.

platen of the tool. While the platen and the chuck are rotating a suspension with Q3 adjusted pH-value of DIW and abrasive particles (slurry) is dispensed on the platen. The abrasive particles are made from silica or ceria with diameters in the 50 nm range. During polishing the particles are accelerated by the micro-pattern of the polishing pad and impinge on the surface of the wafer, thus weakening the strength of the atomic network. The pH-adjusted liquid can penetrate into the weakened network and dissolve atomic clusters from it. Owing to the height variation of the patterned surface a different local pressure is applied to elevated and lower areas of the wafer leading to increased removal on the higher regions. This leads to a planarization of the pattern on a large scale. In Fig. 2 the principle of the removal is presented in detail. In this chapter the emphasis is on surface smoothing by CMP, which can be achieved with a modified CMP planarization process.

Any kind of CMP, however, will lead to a heavy contamination of the polished substrates with particles left on the surface. Since these particles have strong adhesion a special cleaning is an important issue after polishing. Beside soft etching methods and standard cleaning with megasonic agitation we are currently qualifying a special post-CMP cleaner, which scrubs the surface with a soft PVA-brush (polyvinyl alcohol) and remove particles also by mechanical means. Beside the particles a slurry often contains metallic contamination. Thus by including chemistry to the post-CMP cleaning process care has to be taken for lowering the metal contamination down to the stringent levels for CMOS compatible production. It is the aim of this chapter to develop the CMP smoothing and apply it to FBAR to achieve high quality ZnO for resonators and filters.

2
Experimental

We have used 100 mm (100)-oriented silicon wafers as substrates. Wafers with 1–10 Ω cm resistivity were used for structural characterization of the deposited zinc oxide films. High resistivity wafers (>500 Ω cm) were chosen as substrates for processing resonators and filters to eliminate the parasitic effects associated with the semiconducting silicon [4]. Films were sputtered in a cluster tool (Von Ardenne CS 730 S) from 200 mm diameter round targets. In this system metal films are deposited in a multitarget chamber with dc-magnetrons, but to minimize cross-contamination, ZnO is sputtered in a dedicated single target chamber. Reactive dc-magnetron sputtering from zinc target (purity of 99.995%) in argon/oxygen atmosphere is utilized in all experiments. Both gases have purity of 99.9999%. The flow rates of the gases were rationed with massflow controllers and the oxygen content was always set to 41 vol.-%. The loadlocked cluster type sputtering system was pumped with oil free turbodrag and diaphragm pumps to below 5×10^{-5} Pa before sample processing.

Resonators were SMR-type fabricated on quarter wavelength acoustical mirrors, consisting of alternating layers of high (W) and low (SiO_2) acoustic impedance materials. We used a simplified resonator process, where only the top electrode is patterned leaving all other layers (mirror, bottom electrode and ZnO) to cover the whole wafer. Contact to the bottom electrode is done capacitively. The film thicknesses for the resonator stack were calculated by an in-house developed one-dimensional modeling program. Tungsten has the highest known acoustic impedance and the impedance ratio $Z_{high} : Z_{low}$ for W–SiO_2 pair is 7.7 : 1. This ensures good acoustic isolation with only two layer pairs. In case of Mo-SiO_2 the ratio is 4.8 : 1 and consequently one needs an extra pair. Metals were sputter deposited by dc-magnetron and PECVD (plasma enhanced chemical vapor deposition) was used for SiO_2. Our resonator and filter fabrication is explained in more detail elsewhere [4].

Smoothing was done on a Strasbaugh 6 DS-SP planarizer. Standard processing consumables such as pads and slurries were varied in the experiments to achieve the best surface smoothing. Polishing times were varied in the range 30–90 s. Cleaning was done in a batch cleaning in a quartz sink using megasonic agitation for 10 min with pure DIW at 55 °C and subsequent spin-drying for particle removal. Additionally in some cases a SC-1 bath was used for enhanced particle removal.

The film morphology was studied using a digital scanning electron microscope (SEM, Leo 1560). Surface roughness and topology were measured by atomic force microscopy (AFM, Digital Instruments Dimension 3100). FilmTek 4000 spectrophotometry tool was used for optical characterization of ZnO. For electrical characterization of the completed devices Agilent Technologies 8753 network analyzer was utilized.

3
Results and Discussion

Schematic cross sections of the film stacks for both bridge and solidly mounted resonator are shown in Fig. 3. In surface micromachining the air gap is formed by dissolving a sacrificial layer from underneath the bridge, such as copper below silicon nitride bridge [5]. SMR schematic in Fig. 3 has the designed layer thicknesses, whereas the lowest high-Z layer in the actual scanning electron microscopy (SEM) cross section micrograph of a FBAR is too thick. Fortunately it does not affect the mirror performance substantially. This can be deciphered from Fig. 4, which shows the relative calculated displacement amplitude in a resonator

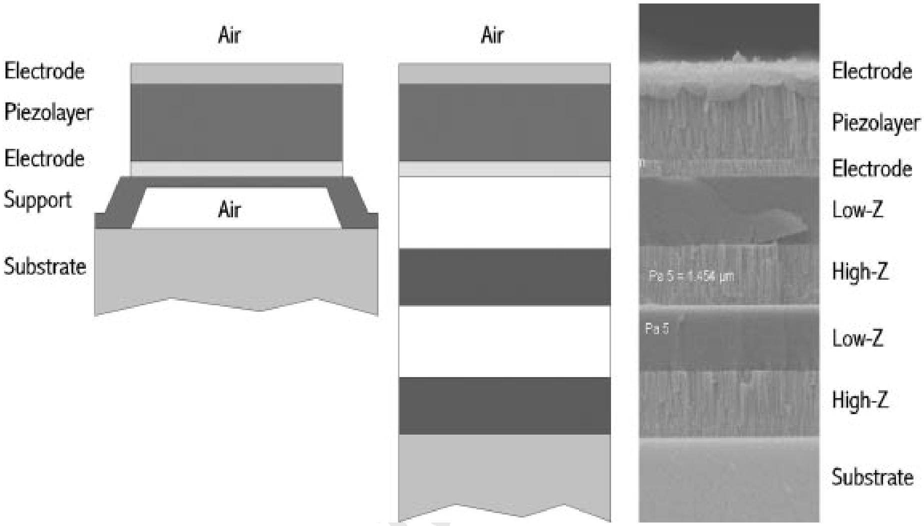

Fig. 3 Bridge and mirror resonator film stacks with cross section SEM of the mirror FBAR.

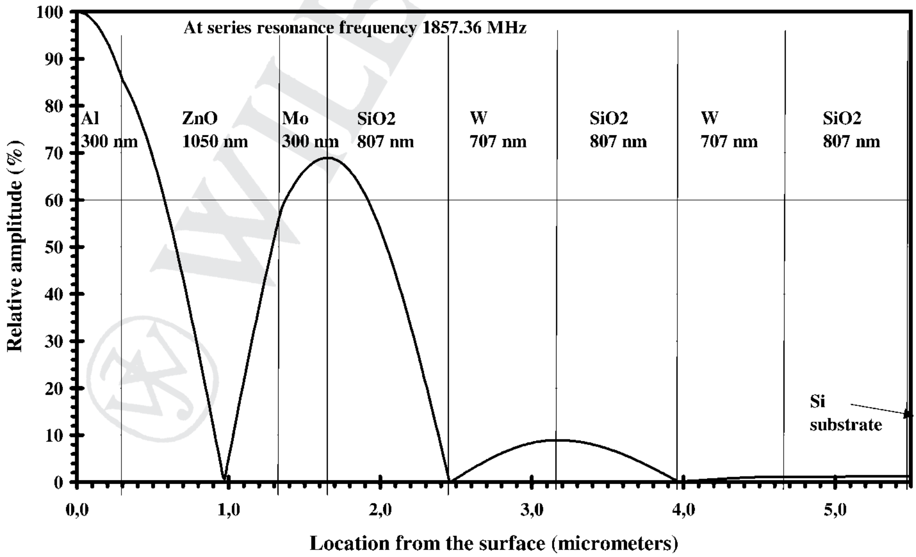

Fig. 4 Relative displacement in a resonator stack at 1857 MHz. Free surface is on the left.

stack with silicon dioxide/tungsten mirror. The relative displacement at the substrate is <2% of the maximum at the series resonance frequency of 1857 MHz; therefore it is not necessary to increase the number of mirror layers in this stack. The highly columnar structure of the metals in the mirror and bottom electrode

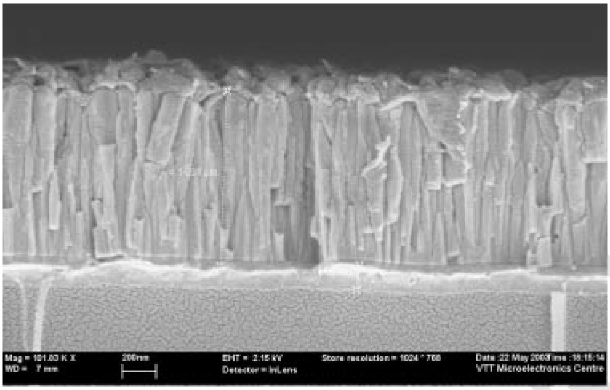

Fig. 5 Cross section SEM micrograph with non-CMP ZnO piezoelectric film on resonator.

is clearly depicted in Fig. 3, as well as the amorphous nature of silicon dioxide. Top electrode is sputtered aluminum and it has been deformed during sample cleaving. The ZnO piezolayer is also highly columnar as desired for strongly preferred orientation. But as can be seen in Fig. 5 the ZnO film on a wafer, which is not CMP, smoothed is porous and the ZnO surface appears to be very rough.

ZnO is transparent, therefore we have measured the samples optically with Filmtek 4000 from ultraviolet to infrared wavelengths (450–1650 nm) [18]. A typical index of refraction (*n*) and extinction coefficient (*k*) as function of the wavelength are shown in Fig. 6. Index of refraction at 633 nm varies on different films from 1.910 to 1.921, which is quite close to the bulk value of 1.997 [19]. In optical respect our ZnO films seem to be of fairly good quality even without CMP smoothing.

It is not feasible to smooth the top electrode metal layer by CMP, due to contamination issues. Gold, one of our electrode materials, is the most feared yield killer in microelectronics. Therefore we decided to smooth the top mirror layer SiO_2 as this is compatible with other work done on our CMP tool. A CMP smoothing process for the silicon dioxide was developed and the topological properties of the films were measured with AFM. As one can see in AFM nanographs in Fig. 7, the surface appearance of PECVD deposited SiO_2 film changes completely in CMP. During the removal of 70–80 nm of oxide by CMP the rms roughness is dramatically reduced from 4–5 nm to <0.3 nm. After the first trials with actual FBAR samples a smooth surface was achieved, but lots of particles were detected on the surface even after post-CMP cleaning. This was resolved by adding a SC-1 cleaning step at 55 °C in the post-CMP cleaning procedure. In the actual FBAR samples we found holes in the oxide. In the overall view the large number of holes can be seen in the optical micrograph (Fig. 8 a), a close up reveals that the holes go through the oxide (Fig. 8 b). This was further confirmed with stylus measurements. It seems that holes originate from defects on the thick tungsten high Z film. These defects in turn cause flaws on the growing SiO_2 and the SC-1 cleaning solution (ammonium and hydrogen peroxide) attacks these resulting in holes.

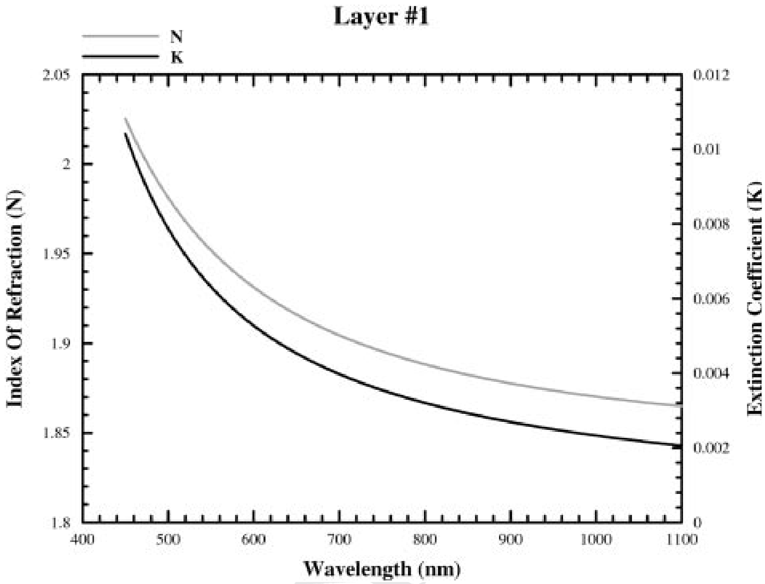

Fig. 6 Filmtek spectrophotometry results of the index of refraction and extinction coefficient as function of wavelength.

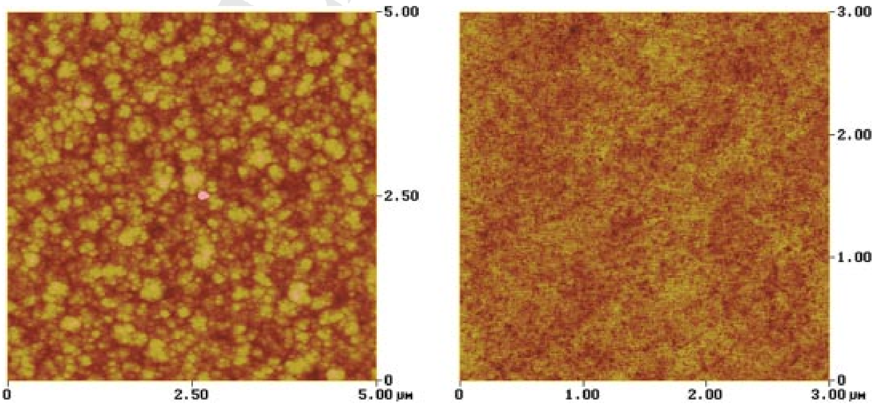

Fig. 7 AFM nanographs of SiO_2: (a) before and (b) after CMP smoothing.

Another issue with CMP smoothing is how our resonator stacks survive through the CMP. This is illustrated in Fig. 9, where a stylus trace (in fact a cross section, compare Fig. 3) of the resonator stack is shown before and after the CMP smoothing. The corners are rounded during CMP, but a large center area of the mirror stack remains flat and uniform. It does seem to be possible to reduce the rounded area further by CMP process development. When including CMP into the FBAR process flow, one has to take into account not only the removal of the

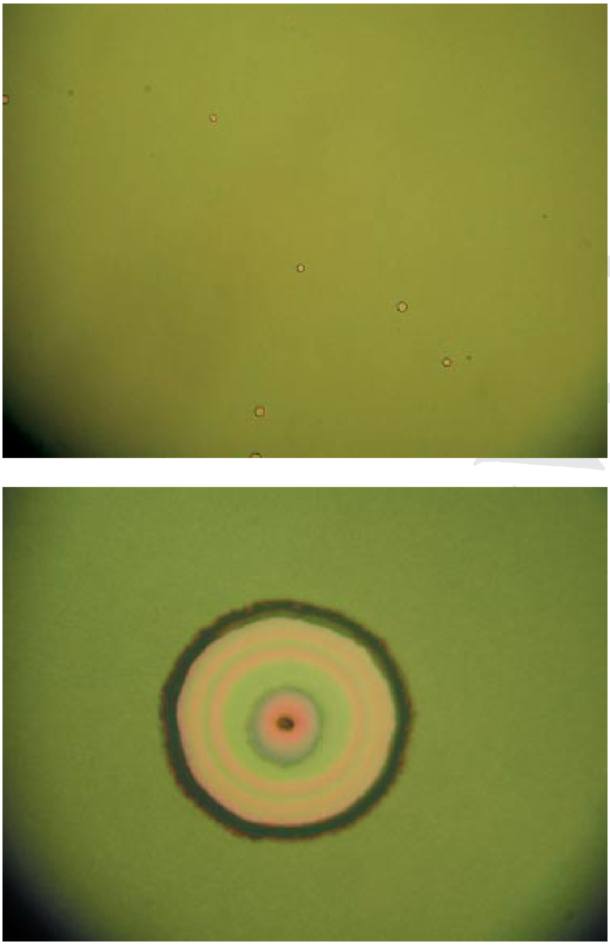

(a)

(b)

Fig. 8 Optical micrograph of SiO_2 surface after post CMP cleaning: (a) overall view, (b) close up of a hole.

oxide by CMP, but also the rounding of the corners by allocating some extra area on the resonator mirrors. Although we loose some chip "real estate" future integration of CMP smoothing into the filter processing seems feasible.

In Fig. 10 AFM nanographs of zinc oxide surface in the old process without CMP smoothing of the silicon oxide and with CMP are shown. Surface roughness has been reduced from 23 to 4.4 nm. The ZnO film (non-CMP) in cross section SEM micrograph in Fig. 5 is from the same sample as in Fig. 10a. The cross section microstructure and surface roughness are also closely related in case of the CMP smoothed ZnO film, where smooth surface also results in dense and featureless SEM cross section (not shown here).

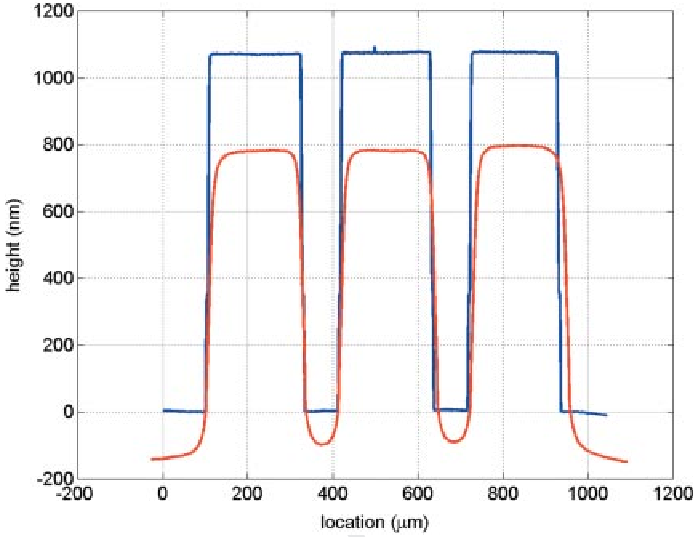

Fig. 9 Dektak stylus trace of the FBAR stack: (a) before and (b) after CMP smoothing.

Smoothing seems to result in better ZnO smoothness as expected and has been reported before [16]. In smoothest ZnO the rms roughness we have achieved with CMP is 4.4 nm, which compares favorably with the best achieved smoothness of non-CMP ZnO, where rms roughness is 13 nm. In a recent work [20] very smooth, rms roughness 1.06 nm ZnO film is reported on an actual SMR FBAR with gold electrodes. ZnO roughness was measured by AFM on the as-deposited samples and it is plotted as function of the deposition run in Fig. 11. Data show that the smoothest ZnO is achieved on those wafers where the top SiO_2 has been smoothed by CMP and the worst roughness was on non-CMP wafers. Another trend is that the ZnO on the non-CMP resonators is getting better with time (more runs). Owing to the instabilities in the ZnO sputter deposition and small number of samples, evidence however is not unambiguous.

The quality of the piezolayer (and the whole resonator) is measured by the effective coupling coefficient and the Q-values at series and parallel resonances. In Fig. 12 the coupling coefficient as function of surface roughness is presented. Two lowest points can be explained by the dc-bias on the substrate during sputtering, which is obviously detrimental to the piezolayer quality. Unfortunately only one CMP-smoothed; wafer survived through the processing (the smoothest one). At the parallel resonance (Qp) Q-values range from 70 to 307, and at the series resonance (Qs) from 69 to 446 without showing any correlation to the ZnO surface roughness. the CMP-smoothed resonator had Qp of 108 and Qs of 339. Due to our simplified resonator process this structure is not optimal for Q-value determination, but nevertheless our Q-values are comparable to the one (201) reported recently [20].

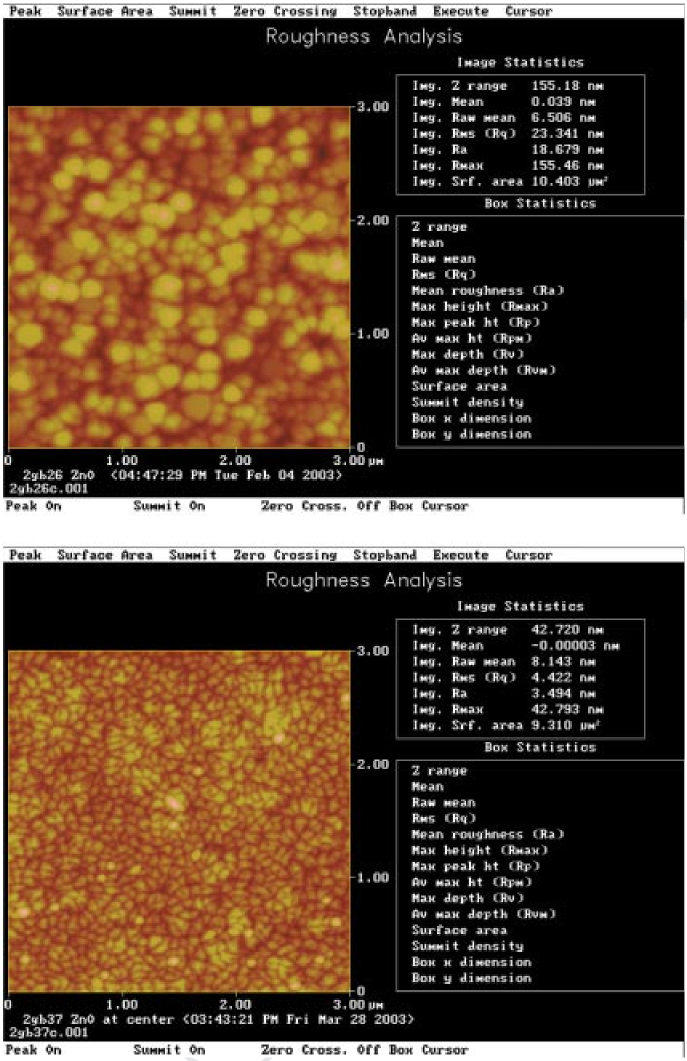

Fig. 10 AFM nanographs of ZnO surface after sputter deposition: (a) non-CMP (b) CMP smoothing applied to SiO_2.

One has to keep in mind that the wavelength of the acoustical waves in ZnO in these resonators is 3 µm, but the scale of the surface roughness is in (tens of) nanometers. Therefore strong physical coupling between the acoustical waves and the surface roughness was not expected. One can speculate that a smoother surface would result in smoother and denser ZnO, because of the effect on film growth during sputtering. This has not been completely verified, as the evidence is inconclusive at this stage.

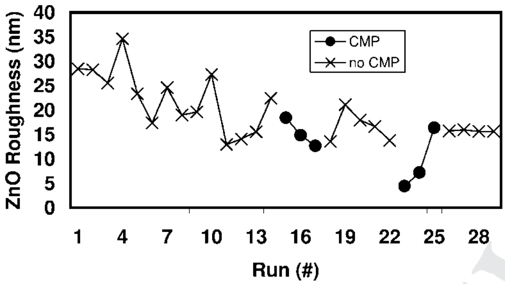

Fig. 11 ZnO surface roughness as measured by AFM after sputtering runs.

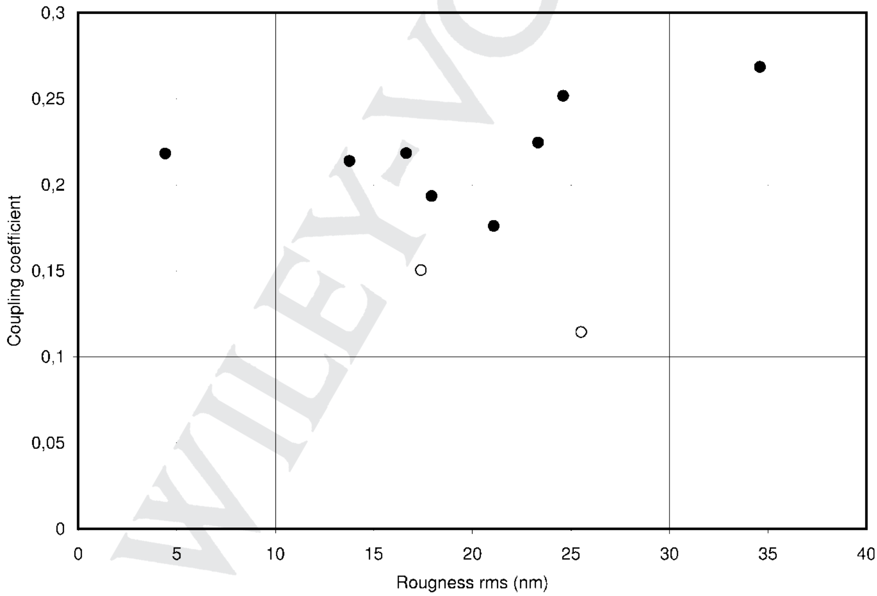

Fig. 12 Acoustic coupling coefficient correlation to ZnO surface roughness. Open circles denote DC-bias on the substrate during sputtering.

4
Conclusions

CMP smoothing was introduced to FBAR (thin film bulk acoustic wave resonator) technology and it was used in fabrication of SMR-type resonators. The ZnO film morphology and microstructure were studied with AFM and SEM, respectively. Optical properties were sampled with spectrophotometry. It was shown that the smoothing of the top mirror SiO_2 improves the surface roughness of the zinc oxide. The roughness achieved with CMP smoothing was 4.4 nm (rms), which compares favorably with 13 nm without CMP. The quality of the ZnO piezolayer was evaluated by measuring the acoustic coupling coefficient and Q-values at parallel and series resonance. ZnO was piezoelectrically good and the CMP smoothing shows good prospects for future integration in FBAR process flow.

Acknowledgments

Special thanks are due to Ms. Meeri Partanen for sample processing and Kimmo Solehmainen for Filmtek measurements.

References

1 Aigner R., Ellä J., Timme H.-J., Elbrecht L., Nessler W., Marksteiner S., in: *Proc. IEEE International Electron Devices Meeting (IEDM)*, San Francisco, 9–11 December **2002**.
2 Lakin K., *IEEE Ultrasonics Symp.* **2002**.
3 Löbl H.P., Klee M., Metzmacher C., Brand W., Milsom R., Dekker R., Lok P., *Mater. Chem. Phys.* **2003**, *79*, 143–146 and *Mater. Sci. Eng. B* **2002**, 1–4.
4 Kaitila J., Ylilammi M., Molarius J., Ellä J., Makkonen T., *IEEE Ultrasonics Symp.* **2001**, 223.
5 Ylilammi M., Ellä J., Partanen M., Kaitila J., *IEEE Trans. Ultrasonics, Ferroelectrics, Frequency Control* **2002**, *49*, 535.
6 Larson III J.D., Ruby R.C., Bradley P.D., Wen J., Kok S.-L., Chien A., *IEEE Ultrasonics Symp.* **2000**, 869.
7 Mansfeld G.D., Kotelyansky I.M., *IEEE Ultrasonics Symp.* **2002**.
8 Newell W.E., *Proc. IEEE* **1965**, *53*, 575–581.
9 Lakin K., Kline G., and McGarron K., *IEEE Trans. Microwave Theory and Techniques* **1995**, *43*, 2933.
10 Molarius J., Kaitila J., Pensala T., Ylilammi M., *J. Mater. Sci.: Mater. Electron.* **2003**, in press. Q4
11 Molarius J., Ylilammi M., US Patent 6,521,100, **2003**.
12 Iriarte G.F., Bjurström J., Westlinder J., Engelmark F., Katardjiev I.V., *IEEE Ultrasonics Symp.* **2002**.
13 Löbl H.P., Klee M., Milsom R., Dekker R., Metzmacher C., Brand W., Lok P., *J. Eur. Ceram. Soc.* **2001**, *21*, 2633–2640.
14 Lee S.-H., Lee J.K., Yoon K.H., *J. Vac. Sci. Technol. A* **2003**, *21*, 1.
15 Lee J.B., Kwak S.H., Kim H.J., *Thin Solid Films* **2003**, *423*, 262–266.
16 Lakin K., Kline G., and McGarron K., *IEEE Ultrasonics Symp.* **1992**, 471–476.
17 *IEEE Standard on Piezoelectricity*, ANSI/IEEE Standard 176, **1987**.
18 US Patent 5 999 267, **1999**.
19 Jellison Jr. G.E., Boatner L.A., *Phys. Rev. B* **1998**, *58*, 3586–3589.
20 Lee J.B., Kim H.J., Soo Gil Kim, Hwang C.S., Hong S.-H., Shin Y.H., Lee N.H., *Thin Solid Films* **2003**, in press. Q5